

Journal of Materials Chemistry C

Accepted Manuscript



This article can be cited before page numbers have been issued, to do this please use: S. Lin, H. Pan, L. Li, R. Liao, S. Yu, Q. Zhao, H. Sun and W. Huang, *J. Mater. Chem. C*, 2019, DOI: 10.1039/C9TC01905G.



This is an Accepted Manuscript, which has been through the Royal Society of Chemistry peer review process and has been accepted for publication.

Accepted Manuscripts are published online shortly after acceptance, before technical editing, formatting and proof reading. Using this free service, authors can make their results available to the community, in citable form, before we publish the edited article. We will replace this Accepted Manuscript with the edited and formatted Advance Article as soon as it is available.

You can find more information about Accepted Manuscripts in the [author guidelines](#).

Please note that technical editing may introduce minor changes to the text and/or graphics, which may alter content. The journal's standard [Terms & Conditions](#) and the ethical guidelines, outlined in our [author and reviewer resource centre](#), still apply. In no event shall the Royal Society of Chemistry be held responsible for any errors or omissions in this Accepted Manuscript or any consequences arising from the use of any information it contains.

ARTICLE

AIPE-active platinum(II) complexes with tunable photophysical properties and the application in constructing thermosensitive probes used for intracellular temperature imagingReceived 00th January 20xx,
Accepted 00th January 20xx

DOI: 10.1039/x0xx00000x

Shengheng Lin,^{‡a} Honghao Pan,^{‡a} Lin Li,^a Rui Liao,^a Shengzhen Yu,^a Qiang Zhao,^c Huibin Sun,^{*a} Wei Huang,^{*a,b,c}

Aggregation-induced phosphorescent emission (AIPE) luminogens based on phosphorescent transition metal complexes have many application advantages in bioimaging compared with fluorescent organic dyes because of their long excitation lifetime and reduced photobleaching. Up to now, however, there are few reports about phosphorescent complexes with AIPE properties, and the reported mechanism of AIPE also needs to be studied in detail. Herein, two series of Pt(II) complexes with different Schiff base ligand structures were designed and synthesized, and all these platinum complexes exhibited obvious AIPE properties. By introducing various electron-rich and electron-deficient functional groups into the Schiff base ligand, the relationship between the AIPE activity and ligand chemical structure was studied in detail. Based on these, a complex with 50% solid-state quantum efficiency has been obtained. Furthermore, one strategy to construct thermoprobes by combining this kind of AIPE-active complexes with thermosensitive N-isopropylacrylamide hydrogel was proposed. The photophysical properties of the resulted thermoprobe were studied in detail in different physiological environment including pH, ionic and amino acid, which show great stability and low cytotoxicity. Finally, the application of this kind of thermoprobe in intracellular temperature distribution imaging was demonstrated.

1 Introduction

Organic luminescent materials have attracted numerous research interests due to their unique optical properties and great application potentials in organic light emitting diodes, data recording and storage, and sensors.¹⁻⁴ However, most of the traditional organic luminescent materials suffer from aggregation-caused quenching (ACQ) in the condensed phase due to the strong dipole-dipole interactions between the organic molecules,^{5,6} which has greatly restricted the applications of organic luminogens in many fields, especially in fluorescent chemosensors and bioimaging in vitro and in vivo.^{7,8} To alleviate or even avoid this phenomenon, many efforts have been made to develop novel organic luminescent materials with solid-state light emission. The more representative works are the aggregation induced emission (AIE) and aggregation

induced emission enhancement (AIEE) effects discovered by Tang and co-workers from a silole dye in 2001, and shortly later by Park and co-workers from cyano-substituted oligophenylenevinyls.^{9,10} Since their initial discovery, libraries of AIEgens have been rationally designed, synthesized, and widely used in various fields.¹¹⁻¹³ To date, most of the established AIEgens are limited to pure organic fluorescent luminogens. As an important kind of organic luminogens, however, phosphorescent AIEgens reported are few with limited examples based on Pt(II), Ir(III), Ag(I) and RE(I) complexes.¹⁴⁻²¹ In fact, it is proverbial that compared with fluorescent luminogens the phosphorescent ones have many application advantages especially in bioimaging since their long excitation lifetime and reduced photobleaching.^{22,23} Therefore, the development of phosphorescent AIEgens and investigation of the underlying AIE mechanisms are important and significant for further enriching the AIE material libraries and practical application.

Phosphorescent transition-metal complexes, especially Pt(II) complexes, have been widely studied in materials science in the past few decades due to their rich spectroscopic and luminescence properties such as much longer emission lifetimes compared with other transition metal complexes, large Stokes shifts, easy color tunability and high photostability.²⁴⁻²⁶ However, for conventional Pt(II) complexes, because of the square planar coordination field and conjugated ligand structure, there always exists Pt-Pt and/or π - π interactions upon excitation in aggregated state, which generate a new metal-metal-to-ligand charge transfer (MMLCT)

^a China Key Laboratory of Flexible Electronics (KLOFE) & Institute of Advanced Materials (IAM), Jiangsu National Synergistic Innovation Center for Advanced Materials (SICAM), Nanjing Tech University (NanjingTech), 30 South Puzhu Road, Nanjing 211816, P.R. China. *E-mail: iamhbsun@njtech.edu.cn; iamwhuang@njtech.edu.cn

^b Shaanxi Institute of Flexible Electronics (SIFE), Northwestern Polytechnical University (NPU), 127 West Youyi Road, Xi'an 710072, China

^c Key Laboratory for Organic Electronics and Information Displays & Institute of Advanced Materials (IAM), SICAM, Nanjing University of Posts & Telecommunications, 9 Wenyuan Road, Nanjing 210023, P.R. China.

† Electronic Supplementary Information (ESI) available: Experimental details. ¹H NMR and Mass spectra. extra absorption and emission spectra. CCDC 1905320. For ESI and crystallographic data in CIF or other electronic format see DOI: 10.1039/x0xx00000x

‡ They contributed to this work equally.

excited state that results in broad and red-shifted emissions in comparison to those of solution state. On the one hand, using the sensitivity of such interactions to external stimuli such as solvents, pH, temperature, biomolecules and so on, Yam and co-workers demonstrated that Pt(II) complexes with terpyridine, 2,6-bis(benzimidazole-2'-yl)pyridine, and 2,6-bis(1-alkylpyrazol-3-yl)pyridine ligands are successful classes of phosphorescent luminogens for the design of functional materials.²⁷⁻²⁹ But on the other hand, these Pt-Pt and/or π - π interactions also often lead to the luminescence performance degradation. Therefore, exploration of novel Pt(II) complexes with aggregation induced phosphorescent emission (AIPE) properties is highly desirable for further expanding their application in luminescent sensors and bioimaging. Up to now, however, only a few Pt(II) platinum complexes with AIPE effects have been reported.³⁰⁻³²

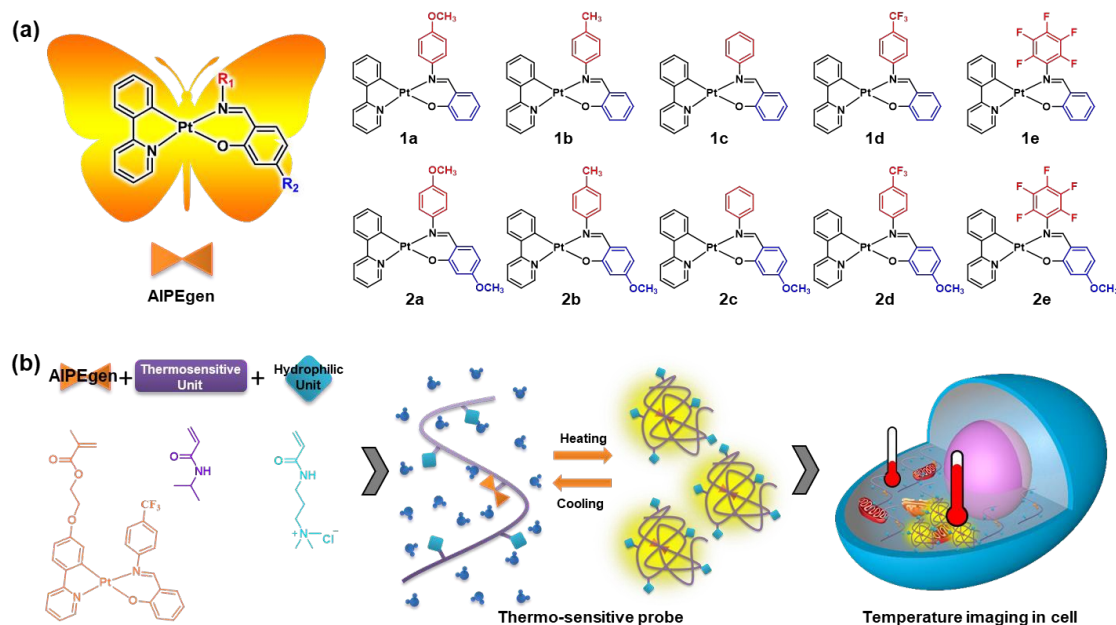
Our group has been extensively working on the design and synthesis of new Ir(III) and Pt(II)-based complexes.³³⁻³⁵ In our previous studies, a class of platinum complexes with AIPE activity based on Schiff base ligands was discovered by chance.³⁰ In continuing our previous work, herein, we have designed and synthesized a new series of Pt(ppy)(LX) type complexes based on Schiff base ligand (LX) structures, aiming at further systematic exploiting the relationship between the Schiff base structures and the AIPE properties including the emission colours, quantum efficiencies, luminescence lifetime and so on (Scheme 1a). Moreover, a new method of constructing phosphorescent thermoprobes by incorporating this kind of AIPE-active Pt(II) complexes into water-soluble acrylamide-based thermosensitive polymers was proposed (Scheme 1b). The phosphorescent polymer **P1** showed weak green emission, which was significantly enhanced upon increasing the temperature from 28 to 40°C because of the conformational changes of polymer chains from an extended structure to an aggregated state, leading to an increase in

rigidity of the microenvironment of the Pt(II) complexes. The photophysical properties of the resulted thermoprobes are studied in detail in different physiological environment including pH, ionic and amino acid, which show great stability and low cytotoxicity. Finally, the application of this kind of thermoprobe in intracellular temperature distribution imaging is demonstrated.

2. Experimental section

2.1 General experimental information

All reagents and chemicals were procured from commercial sources and used without further purification. All solvents were of analytical grade and purified according to standard procedures. ¹H NMR spectra were recorded on a Bruker Ultra Shield Plus 400 MHz spectrometer and chemical shifts were expressed in ppm using Me₄Si as an internal standard. Mass spectra were obtained on a Bruker autoflex matrix-assisted laser desorption ionization time-of-flight (MALDI-TOF) mass spectrometer. The UV-vis absorption spectra were recorded using Shimadzu UV-3600 UV-vis-NIR spectrophotometer. Photoluminescence spectra were measured on an Edinburgh FL 920 spectrophotometer equipped with a temperature controller. Excited-state lifetime studies were performed with an Edinburgh FL920 photcounting system with a semiconductor laser as the excitation source. The absolute quantum yields of the complexes were determined through an absolute method by employing an integrating sphere. The number-average molecular weight (M_n) and weight-average molecular weight (M_w) of the polymers were characterized in THF by GPC at 308 K using polystyrene as standard. The average particle size was measured via DLS on Nano ZS90 with a temperature controller.



Scheme 1 (a) The chemical structures of AIPE-active Pt(II) complexes, (b) Schematic illustration of constructing and temperature distribution imaging cellular cytoplasm thermo-sensitive probe using AIPE-active Pt(II) complexes and thermosensitive hydrogel.

2.2 Synthesis

The Schiff base ligands were synthesized according to a procedure modified from that reported in the literature.³⁶ Generally, an EtOH solution dissolved by salicylaldehyde was added to a stirred EtOH solution of aniline. After adding catalytic amount of AcOH, the reaction mixture was stirred at room temperature for 2 hr. Concentration and subsequent silica gel column purification gave the corresponding ligand. The synthesis of all the Pt(II) complexes was performed according to the same procedure.³⁷ Briefly, Pt(II) μ -dichloro-bridged dimers were synthesized from the starting materials of K_2PtCl_4 and C^N ligand according to the previous report.³⁷ A solution of Pt(II) μ -dichloro-bridged dimers, 3 equiv of the Schiff base ligand and 10 equiv of Na_2CO_3 in 2-ethoxyethanol was heated to reflux for 16 h. Then the reaction mixture was concentrated under reduced pressure. Excess of water was added gradually to give orange or red precipitate of crude product that was subsequently filtered and washed with water. The obtained crude product was purified by silica gel column chromatography, giving the desired complexes in moderate yields. Thermo-sensitive probe **P1** is obtained by general free radical random copolymerization method.³⁸ The detailed synthesis and characterization of all the compounds are provided in the ESI.

2.3 X-ray crystallography

The single-crystal of complex **1e** was obtained from CH_2Cl_2 solution mixed with hexane. And the X-ray diffraction data of complex **1e** were collected on a Bruker Smart Apex CCD diffractometer with graphite monochromated Mo-K α radiation ($\lambda = 0.71073 \text{ \AA}$). All calculations and molecular graphics were carried out on a computer using Mercury software. Crystallographic data (cif files for **1e**) for the structure reported

here have been deposited with the Cambridge Crystallographic Data Center (Deposition No. 1905320)

2.4 Intracellular temperature distribution imaging

The solutions with different pH, amino acids and anions were prepared from the corresponding nitrate salts or hydrochloride salts in deionized water. The in vitro cytotoxicity toward HepG2 cells was measured using the methyl thiazolyl tetrazolium (MTT, Beyotime) assay. HepG2 cell used for imaging were first incubated in culture dishes, washed with PBS three times and then incubated with **P1** 0.01 mg mL^{-1} PBS. Cell imaging experiments were then performed with an Olympus IX81 laser scanning confocal microscope after washing and covered with PBS. After each temperature change, we waited for about 10 min before starting a new measurement.

3 Results and discussion

3.1 Absorption and photoluminescence properties

The UV-vis absorption spectra of all the ten Pt(II) complexes were measured at room temperature in CH_2Cl_2 solution (Fig. 1), and the detailed electronic absorption data are given in Table 1. The shape of absorption spectra of all the complexes in CH_2Cl_2 solution are similar with a relatively wide absorption band and display intense absorption bands below 300 nm with molar extinction coefficients of $\sim 10^4$, which are assigned to the spin-allowed ligand-centered ¹LC (ligand centered) transitions. According to the theoretical calculation results (Table S1, S2 and S3, ESI[†]), the weak absorption bands at about 350–450 nm can be attributed to the spin-allowed ¹MLCT transitions and ¹LLCT transitions and the weak absorption peak over 450 nm can be attributed to spin forbidden ³MLCT and ³LC transitions. These

Table 1. Optical data of platinum complexes series 1 and 2.

Complex	$\lambda_{\text{abs}}(\text{log}\epsilon)/\text{nm}^a$	$\lambda_{\text{em}}/\text{nm}^b$	$\lambda_{\text{em}}/\text{nm}^c$	Φ_{em}^b	Φ_{em}^c	τ^b/ns
1a	260 nm (4.79), 311 nm (4.37), 364 nm (4.13), 402 nm (3.93)	571	567	14%	7%	1484
1b	259 nm (5.13), 309 nm (4.58), 364 nm (4.53), 400 nm (4.31)	578	574	27%	8%	2114
1c	254 nm (4.80), 306 nm (4.30), 364 nm (4.30), 391 nm (4.01), 461 nm (3.48)	566	559	31%	11%	2149
1d	255 nm (4.85), 306 nm (4.30), 364 nm (4.16), 397 nm (3.92), 469 nm (3.60)	580	571	50%	13%	2944
1e	255 nm (5.15), 307 nm (4.57), 364 nm (4.61), 403 nm (4.22), 462 nm (4.01)	617	617	25%	12%	1270
2a	264 nm (4.79), 331 nm (4.24), 364 nm (4.19), 395 nm (4.07), 435 nm (3.95)	552	546	15%	5%	2021
2b	263 nm (4.76), 331 nm (4.18), 364 nm (4.15), 399 nm (4.03), 433 nm (3.90)	578	572	8%	3%	884
2c	260 nm (4.84), 312 nm (4.32), 331 nm (4.23), 363 nm (4.21), 395 nm (4.07), 434 nm (3.92)	536	533	23%	6%	2070
2d	263 nm (4.90), 312 nm (4.37), 331 nm (4.34), 364 nm (4.35), 397 nm (4.14), 431 nm (4.07)	546	541	8%	2%	189 (26.24%) 674 (73.76%)
2e	262 nm (4.98), 311 nm (4.42), 334 nm (4.38), 365 nm (4.51), 405 nm (4.11), 435 nm (3.96)	567	567	13%	7%	1219

^a In CH_2Cl_2 (air-saturated). ^b Pristine crystal. ^c Ground powder.

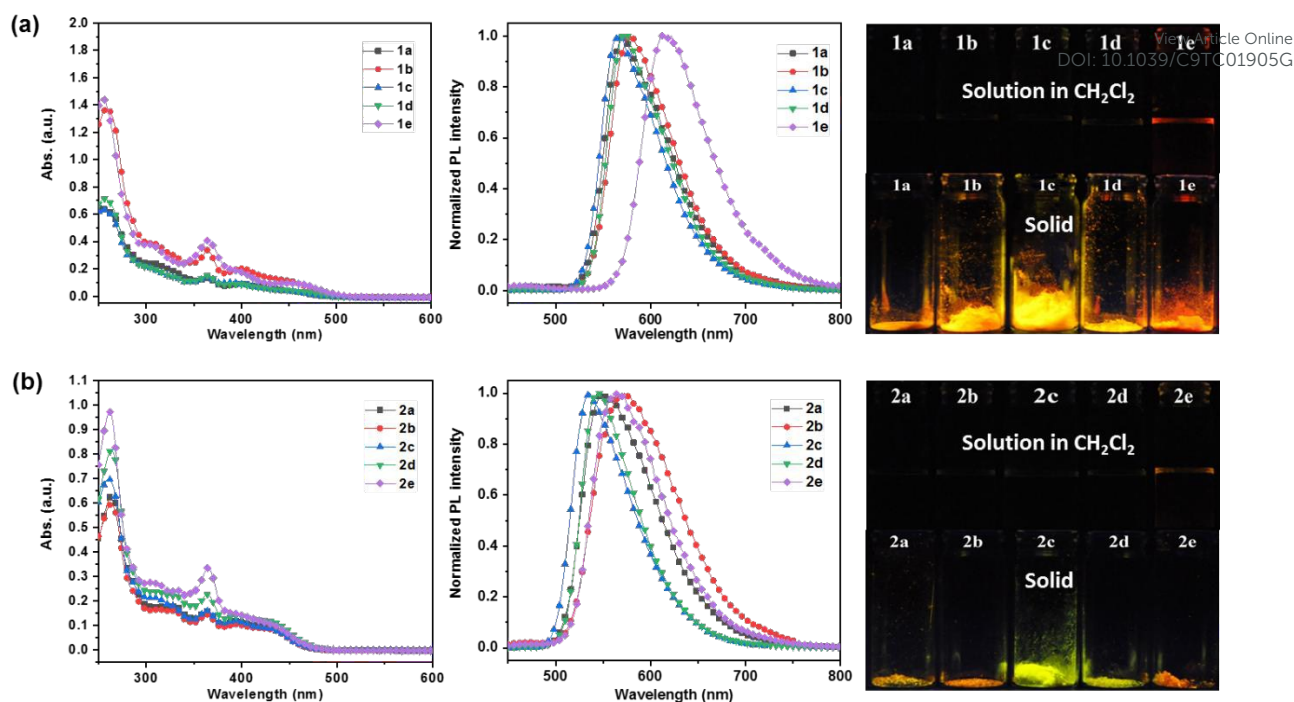


Fig. 1 (a) Absorption spectra in CH_2Cl_2 solution with the concentration of 1×10^{-5} M, photoluminescence spectra in the solid state, and photographs in solution and solid state of series **1** complexes at the room temperature from left to right respectively. (b) Absorption spectra in CH_2Cl_2 solution with the concentration of 1×10^{-5} M, photoluminescence spectra in the solid state, and photographs in solution and solid state of series **2** complexes at the room temperature from left to right respectively.

charge transfer properties of the UV-vis absorption spectra can be further confirmed by the phenomena of UV-vis absorption spectra changing in different solvents (Fig S1 and S2, ESI[†]). The variation in substituents on aniline group of Schiff base ligand caused a negligible effect on the absorption spectra of the complexes. But, interestingly, the change of substituents on *o*-hydroxybenzaldehyde group of Schiff base ligand causing obvious blue-shift of the absorption spectra band-edge of series **2** complexes compared with that of series **1** (Fig. 1). Unconventionally, all the complexes showed no obvious luminescence in dilute solution except for **1e** and **2e**. Although the quantum efficiency of **1e** and **2e** are so low that no obvious emission spectra can be tested, the faint emission can still be seen from their CH_2Cl_2 solution under UV lamp (Fig. 1). This exception may be due to the formation of intramolecular hydrogen bond between the fluorine atom on the aniline group of Schiff base ligand and hydrogen atom on the adjacent ppy ligand, which leads to the molecule more rigid and then partly inhibits the non-radiation transition process caused by the distortion of the molecular structure.

3.2 AIPE properties of the complexes

The room-temperature photoluminescence spectra of all complexes and their images under UV light ($\lambda_{\text{ex}} = 365$ nm) both in solution and pristine crystal state were recorded and shown in Fig. 1. As expected, all complexes exhibit the intense emission at room temperature in solid state. The emission profiles of all complexes in solid state cover a wide range from green to red, reflecting that the modification of Schiff base is effective in tuning the emission color of this kind of AIPE-active complexes.

Among them, **1d** exhibits the strongest crystal-state emission with the absolute quantum efficiency of 50% at room temperature (Table 1). Specifically, for series **1**, except compound **1e**, both the introduction of electron-withdrawing and electron-donating groups on the structure of aniline cause a weak red-shift of the solid-state emission spectra, whereas for series **2** this effect is more obvious. On the contrary, the introduction of electron-donating groups on *o*-hydroxybenzaldehyde group leads to obvious blue-shift of the solid-state emission, which is similar to those of absorption spectra. In addition, compared with the corresponding compounds in series **1**, the complexes of series **2** also exhibit lower quantum efficiency and shorter lifetime. Particularly, **2b** and **2d** exhibit the lowest quantum efficiency and shortest lifetime, which may be due to the Schiff Base and metal centre dominated excited state properties according to the theoretical calculation results (Table S4, ESI[†]).

In order to better show this AIPE phenomenon of all the complexes, herein, a commonly used method to compare the emission intensities of AIPE-active fluorophores in THF- H_2O mixture with different H_2O fractions was adopted. The addition of non-solvent water into the dilute THF solutions can turn on the PL emission of all the complexes (Fig S4, S5, ESI[†]). Taking complex **2c** as an example, as shown in Fig. 2, the PL spectrum in pure THF is undetectable. As the water content increasing from 0% to 40%, the PL spectra of **2c** keep at a low level and show slowly increase. When the water fraction is above 40%, the PL spectra of **2c** in THF- H_2O mixtures are boosted significantly to yield approximately ten-fold enhancement. All the other complexes also show the similar phenomenon (Fig. S4, S5, ESI[†]).

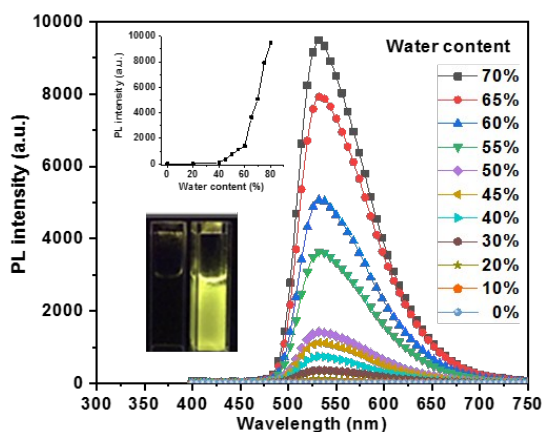


Fig. 2 PL spectra of **2c** in THF/water mixtures with different fractions (f_w). Inset: Variation in relative PL intensity of **2c** with different fractions of water and photographs of **2c** in THF/water with 70% water fractions taken under 365 nm UV light.

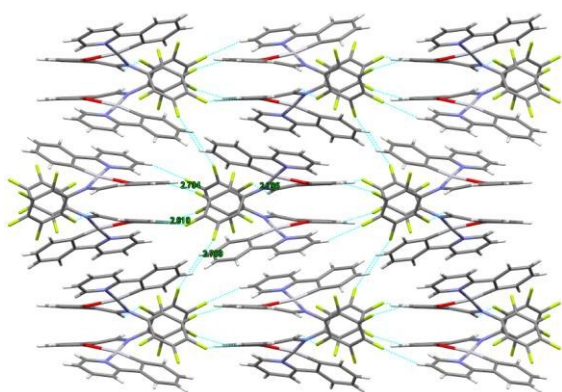


Fig. 3 Intermolecular interactions in **1e** crystal.

The AIPE mechanism of such kind of complexes has been proposed to be the “restricted distortion of excited-state structure (RDES)”, which blocks the non-radiative pathways and generating AIPE activity in the solid state.²⁹ As we all know, the solid-state photoluminescence properties of organic luminescent materials are influenced by two factors, one is the chemical structure of the molecule itself, and the other is the intermolecular interaction determined by the chemical structure of both the luminogens and surrounding media. In order to study the effect of intermolecular interactions on the properties of AIPE in the crystalline state of this kind of complexes, we investigated the changes of photoluminescence spectra of the sample before and after grinding. As shown in Table 1, the maximum emission wavelengths of all complexes, except **1e** and **2e**, show several nanometre blue-shift after grinding, which may be due to the destruction of the weak π - π interactions. And after fully grinding, the quantum efficiency of all complexes showed a significant decrease (Table 1 and Fig. S6 ESI[†]). To further confirm that the AIPE properties comes from RDES other than special intermolecular interactions, solid poly(methyl methacrylate) films doped with different amounts of **2c** were fabricated, which was emissive even at a low content of 0.5% (Fig. S7, ESI[†]).

As previously described, **1e** exhibits special AIPE properties with the longest maximum emission wavelength of 617 nm and

high emission quantum efficiency of 25%. To better understand this phenomenon, the single crystal of **1e** has been obtained from their CH_2Cl_2 solution mixed with hexane and characterized by X-ray crystallography (Table S5, ESI[†]). The molecular packing in crystal-state is depicted in Fig. 3, which shows no evident Pt-Pt and π - π interactions. And this excluded the possibility of the formation of $^3\text{MMLCT}$ states responsible for the crystal-state emission. By the way, there exists obvious multiple hydrogen bonding among the fluorine atoms of aniline and the hydrogen atoms of aromatic ring of the surrounding molecules, showing strong intermolecular interaction, which is possibly the reason why **1e** displays a longer maximum emission wavelength and higher quantum efficiency than other compounds.

3.3 Thermo-sensitive polymer P1

Next, the excellent photophysical properties of this kind of complexes prompted us to study their potential applications in constructing biosensors based on the AIPE characteristics. Herein, we introduced complex **1d** into poly N-isopropylacrylamide backbone a thermosensitive polymer, which can undergo a reversible lower critical solution temperature phase transition between a swollen hydrated state and a shrunken dehydrated state in the temperature range of about 20 to 40°C,³⁹⁻⁴¹ to construct a thermosensitive phosphorescent probe **P1** (Fig. 4, Fig. S8, ESI[†]) via the synergistic effects between the temperature-dependent conformational transition properties of polymer chains and the AIPE properties of the complexes. The detailed synthetic routes of **P1** were shown in ESI, which was mainly composed of three units, including the thermosensitive unit, the hydrophilic unit and the AIPE unit. The photoluminescence response of **P1** in PBS buffer to temperature has been investigated by emission spectral change (Fig. 4a). With increasing temperature from 28 to 38°C, **P1** displayed emission enhancement owing to the increase in rigidity of the microenvironment of the AIPE units caused by the aggregation of polymer chains due to the increase of hydrophobicity. And the dynamic light scattering (DLS) analysis also revealed that the hydrodynamic diameter of **P1** was reduced to 100 nm at 14°C but increased to 700 nm at 38°C (Fig. S9, ESI[†]).

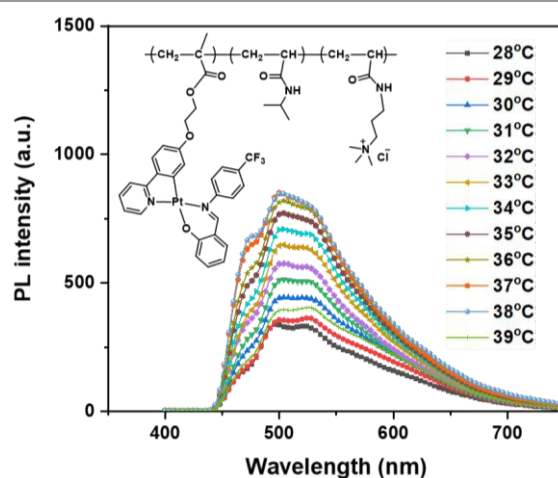


Fig. 4 Emission spectra of **P1** (0.01 w/v%) in PBS (pH = 7.4) at various temperatures. Inset: chemical structure of **P1**.

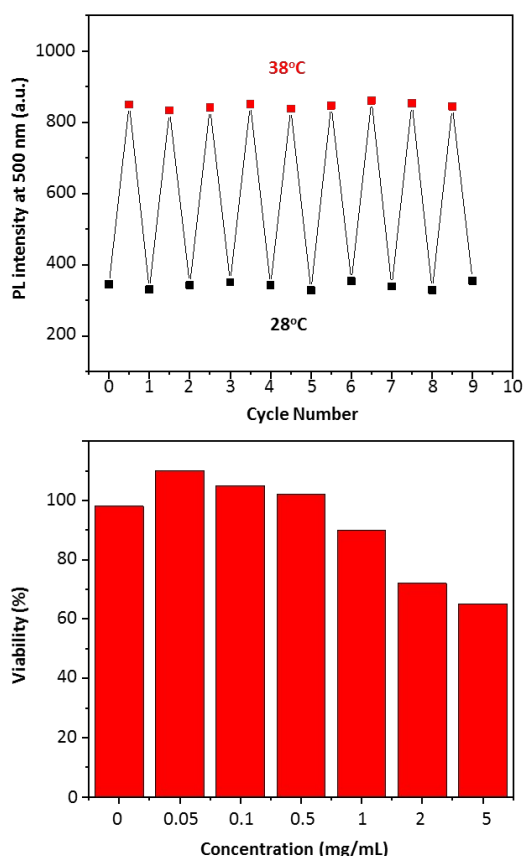


Fig. 5 (a) Reversibility of the luminescence response of **P1** (0.01 w/v%) to temperature variation in PBS. (b) Cytotoxicity of **P1** on HepG2 cells determined by MTT assay.

3.4 The application in intracellular temperature distribution imaging

The potential application of **P1** for intracellular temperature distribution imaging has been evaluated. As shown in Fig. 5a, the luminescence response of **P1** exhibited good reversibility when the temperature was changed between 28 and 38°C repeatedly. Considering that cytotoxicity is a key issue that limits the application of luminescence probes in living organism, the cytotoxicity of **P1** toward HepG2 cells at various concentrations was evaluated by the 3-(4,5-dimethyl-2-thiazolyl)-2,5-diphenyltetrazolium bromide (MTT) assay.⁴² Even if the concentration of **P1** is 0.5 mg/mL and incubated for 2 hr, the cell viability is still close to 100% (Fig. 5b), which demonstrated its good biocompatibility. Besides that, considering the complexity of intracellular environment, further investigation to verify the stability of photoluminescence of **P1** in different intracellular species has been conducted. The experiments demonstrated that **P1** has good stability under different pH, amino acid and ion conditions condition, which also lay the foundation for its application in the field of living cell detection (Fig. S11, ESI[†]).

The use of **P1** for intracellular temperature distribution imaging was demonstrated via confocal laser scanning microscopy upon excitation at 405 nm. The ambient temperature was controlled using a heating stage and digital thermocouple. The colorful imaging of the HepG2 cells labelled

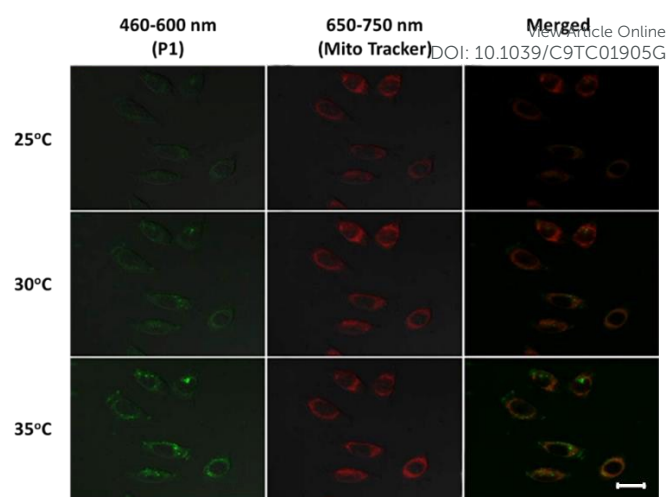


Fig. 6 Confocal laser scanning microscopy images of HepG2 cells labeled with **P1** and Mito Tracker Deep Red at 25°C, 30°C, and 35°C. The green channels were acquired by collecting the luminescence from 450 to 600 nm, while the red channels were from 650 to 750 nm (excitation wavelength was 405nm). Colocalization analysis of Merged ($R = 0.53$). Scale bar = 15 μm .

with **P1** and mitochondrial tracker was collected from two separate channels: 450 to 600 nm of the green channels were acquired by collecting the luminescence from **P1**, while 650 to 750 nm of the red channels were collected from that of mitochondrial tracker. The results showed that **P1** can efficiently internalized by the endocytosis of HepG2 cells and was mainly located in the cytoplasm. The average emission intensity obtained from HepG2 cells after increasing the environmental temperature from 25°C to 35°C is summarized in Fig. 6. The luminescence intensity in the green channel increased with temperature rising, whereas in the red channel changed slightly. Specifically, when HepG2 cells were incubated with **P1** (0.5 mg/ml prepared in fresh media) for 2 hr at 25°C, there was weak phosphorescence emission, and an obvious emission enhancement was observed with increasing temperature from 25 to 35°C. Interestingly, we found that the phosphorescence intensity in different regions of the HepG2 cell is various, indicating that the temperature in the different regions of the cell may be different. By comparing the luminescence position of **P1** and mitochondrial, we further found that these hotspots were mainly distributed around mitochondria, which may be due to the fact that the mitochondrion is the energy provider of the whole cell. The results indicated that **P1** can be used in intracellular temperature distribution imaging.

4. Conclusions

In summary, two series of cyclometalated Pt(II) complexes Pt(ppy)(LX) were successfully synthesized under mild conditions, all of them have significant AIPE properties with long emission lifetime and high solid state quantum efficiency. The emission color could be easily tuned from yellow to red by simply changing the electron withdrawing ability of the substituent group in the N^oO ligands. By studying the emission properties in their solid state, we found all series **2** shown different degree hypochromatic shift and lower quantum

efficiency compared with series **1** because of the existence of methoxyl group at the 4th position of the Schiff base ligand. Particularly, we have developed a novel water-soluble thermosensitive probe **P1** by incorporating this kind of AIPE luminogen in N-isopropylacrylamide hydrogel, which showed good biocompatibility and stability and could be applied to intracellular temperature distribution imaging. To the best of our knowledge, this is the first example of using AIPE luminogen to construct thermosensitive luminescent probe. In the future work, efforts will be made to optimize the polymer configuration and polymerization methods to prepare more efficient and stable high-resolution temperature-sensitive probe.

Conflicts of interest

There are no conflicts to declare.

Acknowledgements

This work was supported by the National Natural Science Foundation of China (21504040). Natural Science Foundation of Jiangsu Higher Education Institutions (15KJB150012). The National Science Foundation of China (81672508). China-Sweden Joint Mobility Project (51811530018). The National Key Basic Research Program of China (973 Program, 2015CB932200). We are grateful to the High Performance Computing Center of Nanjing Tech University for supporting the computational resources.

References

- 1 Y. Shirota and H. Kageyama, *Chem. Rev.*, 2007, **107**, 953-1010.
- 2 Y. Tao, C. Yang and J. Qin, *Chem. Soc. Rev.*, 2011, **40**, 2943-2970.
- 3 L. E. Kreno, K. Leong, O. K. Farha, M. Allendorf, R. P. Van Duyne and J. T. Hupp, *Chem. Rev.*, 2012, **112**, 1105-1125.
- 4 H. Sun, S. Liu, W. Lin, K. Y. Zhang, W. Lv, X. Huang, F. Huo, H. Yang, G. Jenkins, Q. Zhao and W. Huang, *Nat Commun*, 2014, **5**, 3601.
- 5 S. A. Jenekhe and J. A. Osaheni, *Science*, 1994, **265**, 765-768.
- 6 C. Wu, H. Peng, Y. Jiang and J. McNeill, *J. Phys. Chem. B*, 2006, **110**, 14148-14154.
- 7 B. S. Gaylord, S. J. Wang, A. J. Heeger and G. C. Bazan, *J. Am. Chem. Soc.*, 2001, **123**, 6417-6418.
- 8 C.-L. Chiang, S.-M. Tseng, C.-T. Chen, C.-P. Hsu and C.-F. Shu, *Adv. Funct. Mater.*, 2008, **18**, 248-257.
- 9 J. D. Luo, Z. L. Xie, J. W. Y. Lam, L. Cheng, H. Y. Chen, C. F. Qiu, H. S. Kwok, X. W. Zhan, Y. Q. Liu, D. B. Zhu and B. Z. Tang, *Chem. Commun.*, 2001, **18**, 1740-1741.
- 10 B. K. An, S. K. Kwon, S. D. Jung and S. Y. Park, *J. Am. Chem. Soc.*, 2002, **124**, 14410-14415.
- 11 Y. Hong, J. W. Y. Lam and B. Z. Tang, *Chem. Soc. Rev.*, 2011, **40**, 5361-5388.
- 12 J. Wu, W. Liu, J. Ge, H. Zhang and P. Wang, *Chem. Soc. Rev.*, 2011, **40**, 3483-3495.
- 13 J. Mei, Y. Hong, J. W. Y. Lam, A. Qin, Y. Tang and B. Z. Tang, *Adv. Mater.*, 2014, **26**, 5429-5479.
- 14 B. Manimaran, P. Thanasekaran, T. Rajendran, R.-J. Lin, I. J. Chang, G.-H. Lee, S.-M. Peng, S. Rajagopal and K.-L. Lu, *Inorg. Chem.*, 2002, **41**, 5323-5325.
- 15 Y. You, H. S. Huh, K. S. Kim, S. W. Lee, D. Kim and S. Y. Park, *Chem. Commun.*, 2008, **34**, 3998-4000. DOI: 10.1039/C9TC01905G
- 16 P. Alam, G. Kaur, C. Climent, S. Pasha, D. Casanova, P. Alemany, A. R. Choudhury and I. R. Laskar, *Dalton Trans.*, 2014, **43**, 16431-16440.
- 17 M.-X. Zhu, W. Lu, N. Zhu and C.-M. Che, *Chem. Eur. J.*, 2008, **14**, 9736-9746.
- 18 G.-G. Shan, D.-X. Zhu, H.-B. Li, P. Li, Z.-M. Su and Y. Liao, *Dalton Transactions*, 2011, **40**, 2947-2953.
- 19 V. Sathish, A. Ramdass, Z.-Z. Lu, M. Velayudham, P. Thanasekaran, K.-L. Lu and S. Rajagopal, *J. Phys. Chem. B*, 2013, **117**, 14358-14366.
- 20 X.-G. Hou, Y. Wu, H.-T. Cao, H.-Z. Sun, H.-B. Li, G.-G. Shan and Z.-M. Su, *Chemical Communications*, 2014, **50**, 6031-6034.
- 21 Y. Wu, H.-Z. Sun, H.-T. Cao, H.-B. Li, G.-G. Shan, Y.-A. Duan, Y. Geng, Z.-M. Su and Y. Liao, *Chemical Communications*, 2014, **50**, 10986-10989.
- 22 Q. Zhao, C. Huang and F. Li, *Chem. Soc. Rev.*, 2011, **40**, 2508-2524.
- 23 K. Y. Zhang, Q. Yu, H. J. Wei, S. J. Liu, Q. Zhao and W. Huang, *Chem. Rev.*, 2018, **118**, 1770-1839.
- 24 V. H. Houlding and V. M. Miskowski, *Coordin. Chem. Rev.*, 1991, **111**, 145-152.
- 25 V. W. W. Yam, K. M. C. Wong and N. Y. Zhu, *J. Am. Chem. Soc.*, 2002, **124**, 6506-6507.
- 26 W. Y. Wong, G. J. Zhou, X. M. Yu, H. S. Kwok and B. Z. Tang, *Adv. Funct. Mater.*, 2006, **16**, 838-846.
- 27 K. M.-C. Wong and V. W.-W. Yam, *Coordin. Chem. Rev.*, 2007, **251**, 2477-2488.
- 28 C. Y.-S. Chung and V. W.-W. Yam, *Chem. Sci.*, 2013, **4**, 377-387.
- 29 H.-L. Au-Yeung, A. Y.-Y. Tam, S. Y.-L. Leung and V. W.-W. Yam, *Chem. Sci.*, 2017, **8**, 2267-2276.
- 30 S. Liu, H. Sun, Y. Ma, S. Ye, X. Liu, X. Zhou, X. Mou, L. Wang, Q. Zhao and W. Huang, *J. Mater. Chem.*, 2012, **22**, 22167-22173.
- 31 H. Honda, Y. Ogawa, J. Kuwabara and T. Kanbara, *Eur. J. Inorg. Chem.*, 2014, **11**, 1865-1869.
- 32 S. S. Pasha, P. Alam, A. Sarmah, R. K. Roy and I. R. Laskar, *RSC Adv.*, 2016, **6**, 87791-87795.
- 33 Q. Zhao, L. Li, F. Li, M. Yu, Z. Liu, T. Yi and C. Huang, *Chem. Commun.*, 2008, **6**, 685-687.
- 34 X. Mou, Y. Wu, S. Liu, M. Shi, X. Liu, C. Wang, S. Sun, Q. Zhao, X. Zhou and W. Huang, *J. Mater. Chem.*, 2011, **21**, 13951-13962.
- 35 H. Sun, L. Yang, H. Yang, S. Liu, W. Xu, X. Liu, Z. Tu, H. Su, Q. Zhao and W. Huang, *RSC Adv.*, 2013, **3**, 8766-8776.
- 36 C. H. Shin, J. O. Huh, M. H. Lee, and Y. Do, *Dalton Trans.*, 2009, **33**, 6476-6479.
- 37 J. Brooks, Y. Babayan, S. Lamansky, P. I. Djurovich, I. Tsyba, R. Bau, and M. E. Thompson, *Inorg. Chem.*, 2002, **41**, 3055-3066.
- 38 N. Ide and T. Fukuda, *Macromolecules*, 1997, **30**, 4268-4271.
- 39 S. Ito, *Kobunshi Ronbunshu* 1989, **46**, 437-443.
- 40 S. Uchiyama, Y. Matsumura, A. Prasanna de Silva, and K. Iwai, *Anal. Chem.*, 2003, **75**, 5926-5935.
- 41 C. Gota, S. Uchiyama, and T. Ohwada, *Analyst* 2007, **132**, 121-126.
- 42 T. Mosmann, *J. Immunol. Methods* 1983, **65**, 55-63.

Table of Contents

Two series of AIPE-active platinum(II) complexes with tunable photophysical properties were synthesized and their application in constructing thermosensitive probes was demonstrated.

